Oral Microbiology Immunology 2007: 22: 217–224
Printed in Singapore. All rights reserved

ORAL MICROBIOLOGY
AND IMMUNOLOGY

Association of a high-molecular weight arginine-binding protein of *Fusobacterium nucleatum* ATCC 10953 with adhesion to secretory immunoglobulin A and coaggregation with *Streptococcus cristatus*

A. M. Edwards, T. J. Grossman, J. D. Rudney
Department of Diagnostic and Biological Sciences, School of Dentistry, University of Minnesota, Minneapolis, MN, USA

Edwards AM, Grossman TJ, Rudney JD. Association of a high-molecular weight arginine-binding protein of Fusobacterium nucleatum *ATCC 10953 with adhesion to secretory immunoglobulin A and coaggregation with* Streptococcus cristatus. *Oral Microbiol Immunol 2007: 22: 217–224.* © 2007 The Authors. Journal compilation © 2007 Blackwell Munksgaard.

Introduction: *Fusobacterium nucleatum* coaggregates with a diverse range of bacterial species, and binds to host tissues and proteins such as immunoglobulin. These interactions may support the attachment of a variety of organisms to oral surfaces and can facilitate the invasion of soft tissues. We hypothesized that coaggregation with streptococci and immunoglobulin binding may occur by a common adhesin sensitive to L-arginine.
Methods: Repeated mixing of *F. nucleatum* with non-immune secretory immunoglobulin A (S-IgA) and recovery of non-agglutinating cells isolated a spontaneous mutant (isolate 21) of *F. nucleatum* that was defective in S-IgA binding. Wild-type and mutant *F. nucleatum* were compared by coaggregation and adhesion assays.
Results: Isolate 21 exhibited significantly reduced S-IgA binding and coaggregation with oral streptococci but not with *Porphyromonas gingivalis*. Sodium dodecyl sulfate–polyacrylamide gel electrophoresis revealed that the mutant was deficient compared to wild-type for a single protein of approximately 360 kilodaltons. The corresponding protein was isolated from wild-type *F. nucleatum* protein preparations by coprecipitation with arginine–agarose beads. This protein was able to bind both *Streptococcus cristatus* and S-IgA. Mass spectrometry analysis indicated that this protein was closely related to putative autotransporter proteins in other *F. nucleatum* strains and was a 100% match to the deduced amino acid sequence of a 10,638-base-pair open reading frame in the incomplete genome sequence of *F. nucleatum* ATCC 10953. Peptides identified by MS-MS analysis spanned most of the predicted amino acid sequence, suggesting that the mature protein is not subject to postsecretory cleavage.
Conclusion: Coaggregation represents a novel function within the autotransporter class of proteins, which are often associated with virulence.

Key words: autotransporter; coaggregation; *Fusobacterium nucleatum*; immunoglobulin binding; *Streptococcus cristatus*

Joel D. Rudney, Department of Diagnostic and Biological Sciences, School of Dentistry, 17-252 Moos Tower, 515 Delaware Street S.E., Minneapolis, MN 55455, USA
Tel.: +1 612 624 7199;
fax: +1 612 626 2651;
e-mail: jrudney@umn.edu
Accepted for publication September 14, 2006

Interbacterial binding (coaggregation) is believed to be important in the development of dental plaque by facilitating the accumulation of bacteria on surfaces that have already been colonized (28, 38). *Fusobacterium nucleatum* is able to coaggregate with a wide range of oral bacteria and it has been proposed that this plays an indirect role in the progression of periodontitis by forming a bridge between the primary colonizers of the tooth surface (streptococci and actinomyces) and later colonizers such as *Porphyromonas gingivalis*, *Tannerella forsythia* and *Treponema denticola*, which are strongly associated with periodontal disease (28). In addition to facilitating colonization via adhesive interactions, there is evidence that *F. nucleatum* lowers oxygen tension, favoring the growth of proteolytic anaerobes (3). The adhesive properties of *F. nucleatum* are not restricted to bacteria. This bacterium is able to attach to epithelial cells (7, 14, 13, 37, 49, 50), erythrocytes (5, 9, 43, 44) and immune cells (27, 35, 37, 47, 48). Remarkably, although considerable differences in adhesion properties occur between strains, these diverse interactions are often inhibited by either lactose (13, 29, 43), or L-arginine (32, 44, 45, 48).

The soft tissues of the oral cavity are also colonized by a wide range of bacteria (34, 40, 42, 41) and it is likely that, as in dental plaque, coaggregation plays an important role. *F. nucleatum* is able to significantly promote the attachment of *Streptococcus cristatus* to epithelial cells *in vitro* (7). Additionally, bacteria that adhere to invading fusobacteria are carried into host cells (7). Given the diversity of bacteria found within buccal epithelial cells (40, 42, 41), it is likely that complex interbacterial and host–bacterial interactions mediate the colonization of the oral mucosa.

S. cristatus (15, 46) coaggregates strongly with *F. nucleatum* in an L-arginine-sensitive manner (7) and promotes the survival of the anaerobe in saliva (39). As with many oral streptococci, *S. cristatus* produces long fimbriae (4, 15, 16). However, the fimbriae of *S. cristatus* appear to be restricted to certain regions of its cell wall (4, 15, 16). These polar tufts of fimbriae are believed to mediate adhesion both to human cells (7) and to *F. nucleatum* (4, 16, 31). Disruption of a high-molecular weight, serine-rich repeat protein gene by transposon mutagenesis affected the morphology of fimbriae on the surface of the *Streptococcus* and led to reduced coaggregation with *F. nucleatum* (4). In addition, spontaneous mutants that had lost this gene and were defective in fimbriae were abrogated in coaggregation with *F. nucleatum* (16). Despite various studies, the *F. nucleatum* element responsible for coaggregation has not been conclusively elucidated. There is some evidence for the involvement of a protein of approximately 40 kilodaltons (kDa) (23–25), which led to the suggestion of the involvement of the porin protein FomA (20). Another study suggested a high-molecular weight protein of >300 kDa (44). This discrepancy may be the result of inter-strain differences and of the possibility that more than one element is involved. It has also been suggested that FomA mediates fusobacterial adhesion to human immunoglobulin G (10, 11). We hypothesized that coaggregation with streptococci and immunoglobulin binding may occur by a common adhesin that is sensitive to L-arginine. *F. nucleatum* cells were subjected to selection pressures to isolate a spontaneous mutant defective in immunoglobulin adhesion. This mutant was then characterized to determine the protein(s) responsible for immunoglobulin binding and coaggregation.

Materials and methods

Bacterial strains and culture

S. cristatus American Type Culture Collection (ATCC) 49999 (CC5A), *Streptococcus gordonii* DL-1 and *Streptococcus sanguis* SK36 were grown overnight at 37°C in 5% CO_2. *F. nucleatum* subsp. *polymorphum* ATCC 10953 and *P. gingivalis* ATCC 33277 were cultured at 37°C in an anaerobic environment ($N_2 : H_2 : CO_2$, 8 : 1 : 1). Streptococci were cultured in Todd–Hewitt broth (Sigma, St Louis, MO) and both *F. nucleatum* and *P. gingivalis* were cultured in tryptic soy broth (Becton Dickenson, Sparks, MD), supplemented with 0.1% yeast extract (Becton Dickenson), hemin (5 μg/ml; Sigma) and menadione (1 μg/ml; Sigma). Bacteria were recovered by centrifugation (7000 ***g***, 15 min) and washed in phosphate-buffered saline before adjustment to an optical density of 1 at 620 nm ($OD_{620} = 1.0$) in coaggregation buffer (0.001 M Tris–HCl, pH 8.0; 0.1 mM $CaCl_2$; 0.1 mM $MgCl_2$; 150 mM NaCl) (3).

Coaggregation assay

A quantitative assay, based on those described previously (7, 30) was used to measure coaggregation. Magnetic beads (200 μl) precoated with anti-rabbit antibodies (Invitrogen, Carlsbad, CA) were washed three times in coaggregation buffer and incubated for 1 h at 4°C with rabbit polyclonal anti-*F. nucleatum* ATCC 10953 antibodies (diluted 1 : 50). Beads were washed and mixed with 2 ml *F. nucleatum* cells ($OD_{620} = 1.0$, 1 h 4°C). Unbound *F. nucleatum* were removed by washing three times and bead–*F. nucleatum* complexes were resuspended in 400 μl coaggregation buffer. Bead–*F. nucleatum* complexes (20 μl) were added to 0.5 ml streptococci or *P. gingivalis* ($OD_{620} = 1.0$) and incubated with end-over-end rotation for 30 min at 37°C). When inhibitors were used, bead–*F. nucleatum* complexes were preincubated with the inhibitor for 15 min before use. Concentrations of inhibitor were maintained during the assay. After coaggregation had been allowed to occur *F. nucleatum*–bead–partner bacteria coaggregation complexes were removed with a Dynal MPC®-S magnetic stand (Dynal Biotech ASA, Oslo, Norway). The optical density of the remaining bacteria was compared with the starting value. This allowed the number of bacteria bound to *F. nucleatum* to be determined. Results were expressed as % coaggregation. This was determined as the number of bacteria bound to *F. nucleatum*–bead complexes as a percentage of the starting value.

Immunoglobulin-binding assay

F. nucleatum cells were washed three times in coaggregation buffer and resuspended to $OD_{620} = 1.0$. Aliquots (1 ml) were mixed with 5 μg purified immunoglobulin (Sigma) and mixed by end-over-end rotation at 37°C for 30 min in 2-ml centrifuge tubes. For visual assays, mixtures were transferred at this point to glass test tubes and left to stand for 1 h at room temperature.

For quantitative assays, three rounds of washing removed unbound secretory immunoglobulin A (S-IgA) before the addition of magnetic beads (10 μl) coated with anti-S-IgA antibodies (Sigma).

These were prepared as follows; anti-rabbit immunoglobulin G (IgG)-coated magnetic beads (200 μl) were washed three times in coaggregation buffer and resuspended in 500 μl of 1 : 50 dilution of rabbit anti-human IgA before end-over-end rotation at 4°C for 1 h. Beads were washed three times and resuspended to a final volume of 200 μl. *F. nucleatum* that had been incubated with S-IgA and washed were mixed with beads by end-over-end rotation as described (at 37°C for 30 min). *F. nucleatum* cells that had bound

S-IgA became fixed to the beads and were removed by magnetic separation. These assays were performed in the presence or absence of various inhibitors, as indicated in the *Results* section. *F. nucleatum* cells were preincubated with inhibitor for 15 min before use.

Simple measurement of the optical density of *F. nucleatum* suspensions in the presence or absence of S-IgA–bead complexes allowed an accurate determination of S-IgA-binding, expressed as % agglutination (% input *F. nucleatum* bound to S-IgA–bead complexes).

Selection of a spontaneous S-IgA binding-deficient *F. nucleatum* mutant

The selection of a spontaneous *F. nucleatum* mutant that is defective for S-IgA binding has been described previously (7). Briefly, *F. nucleatum* cells (10^8) were mixed with purified S-IgA (0.05 mg/ml; Sigma) by vortexing for 30 s at room temperature, leading to agglutination of the bacteria. Agglutinated cells were allowed to settle and the supernatant was recovered and cultured as described. This procedure was repeated 10 times before supernatants were plated on trypticase–soy–yeast agar supplemented with hemin and menadione. Individual colonies were assessed for S-IgA binding by dot blot and agglutination in the presence of S-IgA. Isolate 21 was selected for on the basis of deficiency in S-IgA binding.

Purification of arginine-binding protein

Cells from stationary-phase cultures of *F. nucleatum* (20 ml) were pelleted by centrifugation and washed three times in coaggregation buffer. Bacteria were resuspended in 4 ml coaggregation buffer supplemented with octyl-β-D-glucopyranoside (100 mM) and protease inhibitors (Sigma) and incubated with end-over-end rotation at 4°C for 18 h. Cell debris was removed by centrifugation (21,000 ***g*** for 20 min) and the supernatant was mixed with L-arginine–agarose beads (VWR Scientific, West Chester, PA; 0.5 ml, washed three times in coaggregation buffer). The supernatant/bead slurry was mixed with end-over-end rotation at 4°C for 16 h. Beads were recovered using a polystyrene chromatography column (VWR Scientific) and washed with 10 volumes of coaggregation buffer. Bound protein was eluted from the beads with four 1-ml aliquots of L-arginine (150 mM in coaggregation buffer). Fractions were dialyzed against double-distilled H_2O and concentrated by freeze-drying. Elutions were resuspended in coaggregation buffer and checked for purity by sodium dodecyl sulfate–polyacrylamide gel electrophoresis (SDS–PAGE) and their concentration was determined by the Coomassie protein concentration assay (Pierce, Rockford, IL).

Protein analysis

Denaturing SDS–PAGE was performed using 8% acrylamide gels run at 120 V for 2.5 h. Proteins were stained with Coomassie blue. Bands of interest were cut from stained gels with a scalpel and sent to the Center for Mass Spectrometry and Proteomics, University of Minnesota for analysis. Peptides were generated by in-gel digestion with trypsin and desalted using reverse-phase chromatography (ZipTip, Millipore Corp. Billerica, MA) before analysis by matrix-assisted laser desorption ionization–time of flight (MALDI-TOF) with a QStar XL mass spectrometer. Peptide data were screened against all bacterial protein sequences in GenBank and likely peptides were deduced.

Sequence analysis and genomics

To identify the gene encoding arginine-binding protein we screened peptide sequences against the deduced amino acid sequences from large open reading frames in *F. nucleatum* genomes. To date, the genomes of two subspecies of *F. nucleatum* have been completed (subsp. *nucleatum* and subsp. *vincentii*; 21, 22). The third subspecies, *polymorphum*, is currently being sequenced (http://www.hgsc.bcm.tmc.edu/projects/microbial/Fnucleatum). However, the latest assemblies are available for download. The largest (approx. 2,400,000 base pairs) was examined for open reading frames using ORF fiNDER (NCBI, http://www.ncbi.nlm.nih.gov/gorf/gorf.html). Open reading frames that may code for proteins of mass >250 kDa were considered as candidates. The deduced amino acid sequence of each was screened against peptide sequences. Deduced amino acid sequences were also screened with the conserved domain database (http://www.ncbi.nlm.nih.gov/Structure/cdd/cdd.shtml, 36) and against other proteins using BLAST (1).

Enzyme-linked immunosorbent assay

Purified arginine-binding protein was solubilized in coating buffer (19) (1 μg in 50 μl/well) and used to coat microtiter wells. Excess protein binding sites were blocked with 3% bovine serum albumin before the addition of S-IgA or *S. cristatus*. Bound S-IgA was detected with rabbit anti-human S-IgA antibodies (1 : 5000) and then alkaline phosphatase-conjugated anti-rabbit antibodies (1 : 5000). Bound *S. cristatus* were detected with polyclonal anti-*S. cristatus* antibodies (1 : 5000) and alkaline phosphatase-conjugated anti-rabbit antibodies (1 : 5000). The anti-*S. cristatus* antibodies had been found not to cross-react with *F. nucleatum* in a previous study (7) so control wells contained only bovine serum albumin with primary and secondary antibodies (which was also the case for the S-IgA binding enzyme-linked immunosorbent assay). Wells were developed with a chromogenic substrate and absorbance was measured with a spectrophotometer (490 nm). Specific binding was determined by subtracting the absorbance of the controls.

Dot blot

Dot blots were employed using whole bacteria or purified protein. Either 3 μl washed *F. nucleatum* ($OD_{620} = 1.0$) or purified arginine-binding protein (0.5–2 μg) was suspended in coaggregation buffer (200 μl) and spotted onto nitrocellulose using a vacuum manifold. Membranes were blocked with bovine serum albumin (3%) overnight at 4°C before incubation with purified immunoglobulin (5 ng/ml) at room temperature for 1 h. Bound immunoglobulin was detected by anti-human IgA or IgG conjugated to alkaline phosphatase (Sigma; diluted 1 : 3000 in coaggregation buffer) and incubation in Sigmafast™ alkaline phosphatase detection solution (Sigma). Control blots received only detection antibodies.

Scanning electron microscopy

Coaggregates were allowed to form as described above and 50 μl was transferred by pipette onto coverslips coated with poly-L-lysine. After 10 min, excess liquid was removed, the slides were washed and bound bacteria were fixed with 2% glutaraldehyde in 0.1 M sodium cacodylate buffer, (pH 7.4 with 0.15% alcian blue 8GX) for 1 h (8). Samples were washed in 0.1 M cacodylate buffer (5 min) followed by secondary fixation (1% osmium tetroxide in 0.1 M cacodylate buffer, 1 h). Samples were washed with 0.1 M cacodylate buffer (5 min) followed by dehydration with ethanol and critical-point drying. Dehydrated samples were coated

for 12 min with platinum using an Ion Tech argon ion beam coater and imaged on a Hitachi S-4700 field emission scanning electron microscope operated at 5 keV.

Statistics

Statistical analyses were performed using Student's *t*-test. Values that were statistically different from controls are indicated in the figures by an asterisk. Error bars indicate the mean ± standard deviation of three independent experiments performed in triplicate.

Results

F. nucleatum coaggregation with oral streptococci and binding to S-IgA are both inhibited by L-arginine

F. nucleatum cells agglutinated in the presence of purified S-IgA but not plasma IgA (P-IgA) or plasma IgG (P-IgG) (Fig. 1A). Agglutination was significantly reduced in the presence of L-arginine (10 mM) (Fig. 1B,C). Lactose (50 mM) slightly decreased agglutination but this was not statistically significant. EDTA (1 mM) inhibited agglutination but not to the same extent as L-arginine (Fig. 1B,C). S-IgA binding was not affected by lysine or serine (10 mM) or by mannose (50 mM) (data not shown).

Coaggregation between *F. nucleatum* and *S. cristatus* was significantly inhibited by L-arginine (10 mM, Fig. 1C), but was only slightly affected by lactose or EDTA (Fig. 1C). Similar results were observed with *S. gordonii* and *S. sanguinis* (data not shown). Coaggregation between *F. nucleatum* and *S. cristatus* was not affected by pretreatment with S-IgA, P-IgA or P-IgG but was inhibited by polyclonal anti-*F. nucleatum* immune serum (Fig. 1D). Analysis of coaggregation by scanning electron microscopy confirmed that *S. cristatus* attached to fusobacteria via polar tufts of fibrils. However, similar structures were not observed on *F. nucleatum* cells (Fig. 2), and there were no morphological differences between wild-type and isolate 21 cells (data not shown).

To determine if the inhibitory effect of L-arginine on S-IgA binding was specific or not, we preincubated *F. nucleatum* with the amino acid before incubation with immune serum. Anti-*F. nucleatum* agglutinated the fusobacteria in the presence or absence of L-arginine (data not shown).

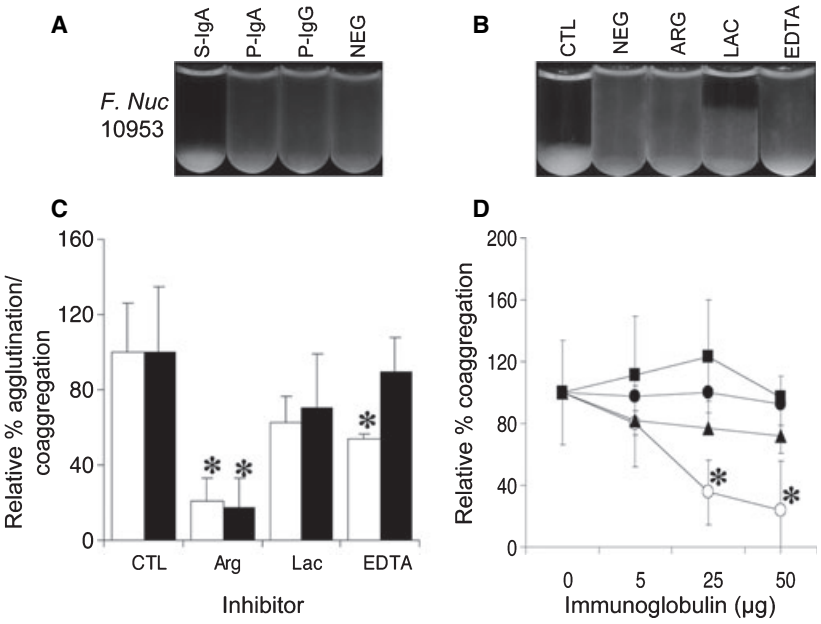

Fig. 1. Effect of L-arginine, lactose or EDTA on *Fusobacterium nucleatum* S-IgA-mediated agglutination and coaggregation. (A) Agglutination of *F. nucleatum* in the presence of human immunoglobulin. (B) Effect of L-arginine, lactose or EDTA on S-IgA-mediated *F. nucleatum* agglutination. Bacteria in the absence of S-IgA are shown for comparison (NEG). (C) Quantitative depiction of the inhibition profiles for *F. nucleatum* agglutination by S-IgA (white bars) and coaggregation with *Streptococcus cristatus* (black bars). Bars with asterisks denote a statistically significant difference ($\alpha = 0.05$) from their respective controls (*F. nucleatum* with S-IgA or *S. cristatus*, without inhibitors). (D) Inhibitory effect of purified human immunoglobulin or immune serum on *F. nucleatum* coaggregation with *S. cristatus*. The treatments used were S-IgA (squares), P-IgA (closed circles), P-IgG (triangles), anti-*F. nucleatum* sera (open circles). The asterisks denote statistical significance at $\alpha = 0.05$.

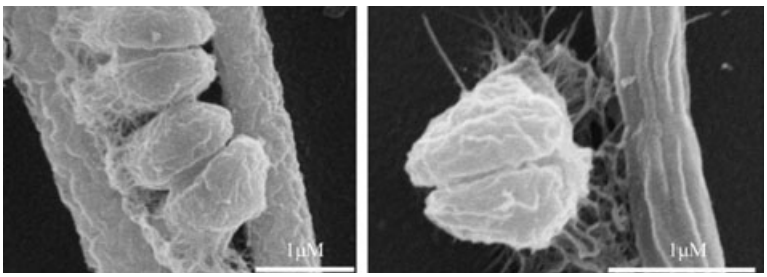

Fig. 2. Scanning electron micrographs of coaggregation between *Fusobacterium nucleatum* and *Streptococcus cristatus*. The use of the cationic dye alcian blue allows the visualization of fine structures (fibrils) that mediate attachment of *S. cristatus* to *F. nucleatum*.

A spontaneous mutant of *F. nucleatum* is defective in S-IgA binding and coaggregation with oral streptococci

Because *F. nucleatum* agglutinated strongly in the presence of S-IgA we were able to select for spontaneous mutants that were defective in S-IgA binding. Repeated selection yielded isolate 21. This isolate displayed reduced agglutination in the presence of S-IgA (80% reduced compared with wild-type, Fig. 3A).

Wild-type *F. nucleatum* cells coaggregated strongly with oral streptococci and *P. gingivalis* (Fig. 3A). However, the coaggregation of isolate 21 with the oral streptococci was significantly reduced relative to wild-type (Fig. 3A). Coaggregation of isolate 21 with *P. gingivalis* was similar to that of wild-type cells (Fig. 3A). Binding of bacteria with P-IgA or P-IgG was similarly affected; isolate 21 exhibited reduced binding relative to wild-type cells (Fig. 3B). S-IgA, P-IgA and P-IgG all bound strongly to immobilized wild-type bacteria (Fig. 3B), suggesting that the lack of agglutination by P-IgA and P-IgG (Fig. 1D) was the result

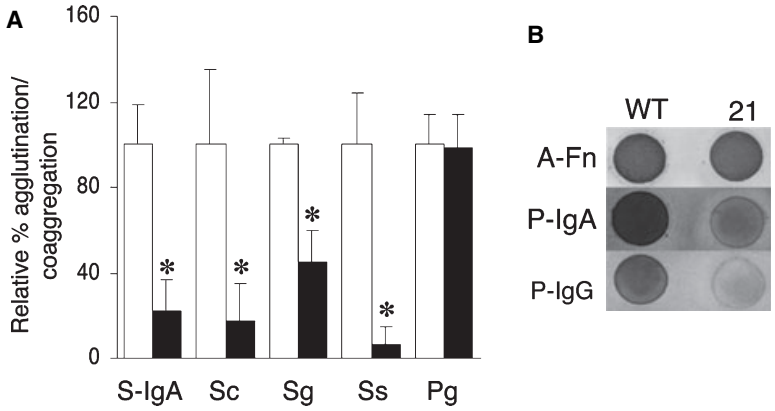

Fig. 3. Binding profile of isolate 21 relative to WT *Fusobacterium nucleatum*. (A) Binding of secretory immunoglobulin A (S-IgA) or *Streptococcus cristatus* (Sc), *Streptococcus gordonii* (Sg), *Streptococcus sanguinis* (Ss) or *Porphyromonas gingivalis* (Pg) by wild-type *F. nucleatum* (open bars) or isolate 21 (solid bars). (B) Reactivity of wild-type *F. nucleatum* or isolate 21 with rabbit polyclonal anti-*F. nucleatum* immune serum (A-Fn) and binding of human P-IgA or P-IgG (5 ng/ml).

of their monomeric structure and not the lack of a receptor for those immunoglobulins. In contrast, isolate 21 exhibited reduced binding of all immunoglobulins (Fig. 3B), suggesting that it might be deficient in a common immunoglobulin receptor.

A high-molecular weight arginine-binding protein is absent in isolate 21

Total proteins from wild-type or isolate 21 *F. nucleatum* were extracted and examined by denaturing SDS–PAGE. Isolate 21 was deficient in a single high-molecular-weight protein of approximately 360 kDa (Fig. 4). This protein could be recovered from octyl-β-D-glucopyranoside-extracted wild-type *F. nucleatum* proteins by coprecipitation with arginine–agarose beads (Fig. 4) and was thus termed arginine-binding protein.

Purified arginine-binding protein supports attachment of *S. cristatus* and S-IgA

Purified arginine-binding protein was immobilized onto microtiter wells, blocked with bovine serum albumin and incubated with S-IgA or *S. cristatus*. Both S-IgA and *S. cristatus* bound to purified arginine-binding protein in a dose-dependant manner (Fig. 5A,B). In addition, arginine-binding protein was immobilized onto nitrocellulose and tested for reactivity with polyclonal antibodies raised to whole cells of *F. nucleatum* 10953 and for binding to P-IgA and P-IgG. The polyclonal antisera reacted strongly with arginine-binding protein, and the immobilized protein bound both P-IgA and P-IgG. Similar dot blot results were obtained for S-IgA binding (not shown). Binding of rabbit anti-human IgA and anti-human IgG (detection antibodies) was minimal (Fig. 5C).

Identification of arginine-binding protein

MS-MS analysis of arginine-binding protein yielded several peptides that were near-identical matches with predicted outer membrane proteins from the sequenced genomes of *F. nucleatum* subsp. *vincentii* and *F. nucleatum* subsp. *nucleatum* (Table 1).

Accession numbers of the closest match to each peptide are indicated, either a *F. nucleatum* subsp. *vincentii* outer membrane protein or *F. nucleatum* subsp. *nucleatum* outer membrane protein. The sequence of the deduced peptides and their position within the predicted arginine-binding protein amino acid sequence are indicated.

The genome of *F. nucleatum* ATCC 10953 is not yet complete but the most recent assembly revealed five open reading frames >8000 base pairs. The predicted peptide sequence of each one was screened against the peptide sequences derived from MS-MS analysis. All of the peptides were a 100% match with the predicted peptide sequence of a 10,638-base-pair open reading frame.

This was the second largest open reading frame identified in the downloaded DNA sequence. The predicted mass of this protein was 370 kDa, which is in keeping with the size estimated by SDS–PAGE. Three open reading frames of unknown function precede *abp* (the gene for arginine-binding protein) with *sec*Y before these. Four genes on the opposite strand are found downstream of *abp*, ribosome recycling factor (*rrf*), uridylate kinase (*pyr*H), elongation factor (EF_TS) and ribosomal protein S2 (R_S2). The precise location of the arginine-binding protein open reading frame on the genome is unknown because sequencing is not yet complete.

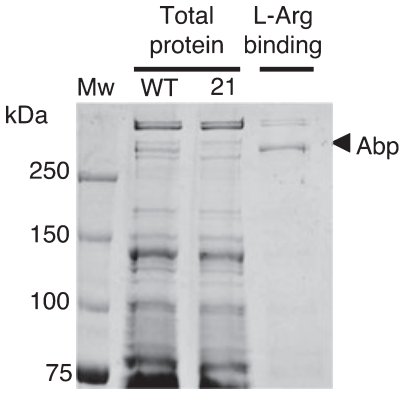

Fig. 4. Total protein profile of isolate 21 compared with wild-type *Fusobacterium nucleatum* and protein recovered by L-arginine–agarose beads from solubilized wild-type *F. nucleatum* preparations (arrow).

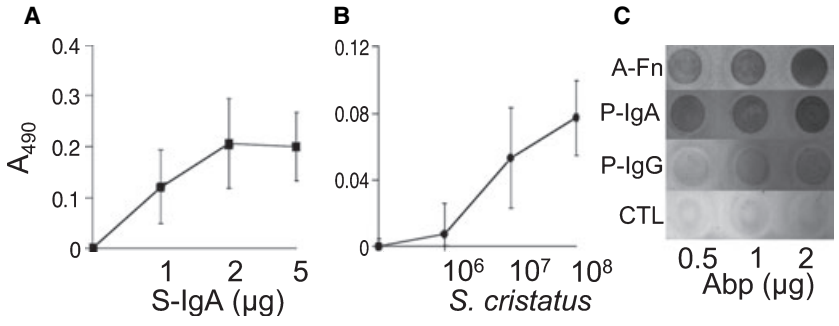

Fig. 5. Binding profile of purified arginine-binding protein. (A) Binding of S-IgA to immobilized arginine-binding protein. (B) Binding of *Streptococcus cristatus* to immobilized arginine-binding protein. (C) Reactivity of arginine-binding protein with rabbit anti-*Fusobacterium nucleatum* polyclonal immune serum and binding of human P-IgA and P-IgG. Similar dot blot results were obtained for S-IgA binding (not shown). CTL is a blot incubated with rabbit anti-human detection antibodies only.

Table 1. Peptides generated by MS-MS analysis

Accession no.	Protein	Sequence	Position
gi|34762267	Fnv OMP	IEKEQENISQMLK	56–68
gi|34762267	Fnv OMP	GEFWVKPLEK	88–97
gi|34762267	Fnv OMP	YYGEYGIVK	144–152
gi|34762267	Fnv OMP	NPLEFVDK	153–160
gi|34762267	Fnv OMP	IDFGANITPK	161–170
gi|34762265	Fnv OMP	NNIYLFAQGSR	1493–1503
gi|34762265	Fnv OMP	LVGMFFDNSAAQTK	2265–2278
gi|19704858	Fnn OMP	DFNISLGTNAK	2281–2291
gi|34762265	Fnv OMP	SAEGIGMYAK	2446–2455
gi|19704858	Fnn OMP	VNLTGDLSVASGDSK	2634–2648
gi|19704858	Fnn OMP	NSIGIFGDNSNINFK	2905–2919
gi|34762265	Fnv OMP	VDTNVYTNATK	2980–2990
gi|19704858	Fnn OMP	SISGVAEVLPNFSK	3104–3117
gi|34762265	Fnv OMP	NLASGLEDIR	3184–3193
gi|34762265	Fnv OMP	FSVIYTGGEHK	3263–3273
gi|34762265	Fnv OMP	STGVLYLNDR	3286–3295
gi|34762265	Fnv OMP	YSQVGADTYQNK	3369–3380
gi|34762265	Fnv OMP	GKDYFVITPNVGVETK	3435–3450
gi|34762265	Fnv OMP	DYFVITPNVGVETK	3437–3450
gi|34762265	Fnv OMP	NASTGYYDLSKPER	3487–3500
gi|19704858	Fnn OMP	VAVGAELGLEK	3505–3515

Accession numbers of peptide matches are indicated along with the inferred sequence. Each peptide was found in an outer-membrane protein (OMP) of *Fusobacterium nucleatum* subsp. *nucleatum* (Fnn) or *F. nucleatum* subsp. *vincentii* (Fnv). The positions of these peptides within the deduced amino acid sequence of arginine-binding protein are also shown.

Analysis with the conserved domain database (36) suggested that arginine-binding protein is a member of the autotransporter family of proteins. Sequence analysis revealed that arginine-binding protein has several properties common to this group of proteins, including a long signal peptide, an RGD motif, a C-terminal β-barrel and a C-terminal YXF motif (18, 17). Homologous open reading frames, were found in the two sequenced subspecies (subsp. *vincentii*: 2961 residues, 78.8% homology, 64.9% identity; subsp *nucleatum*: 2143 residues, 82.9% homology, 49.9% identity). Both of these open-reading frames code for proteins with RGD and C-terminal YXF motifs and C-terminal β-barrels.

Many autotransporters cleave the N-terminal part of the mature protein (passenger domain) upon reaching the bacterial cell surface (18, 17). However, the peptides derived from MS-MS analysis spanned almost the whole protein, starting just 15 residues from the probable signal peptidase site, ruling out similar cleavage of arginine-binding protein.

Discussion

The oral cavity is host to a diverse array of bacteria, which colonize the many different surfaces of the mouth. Such an environment supports a multitude of host–bacterial and inter-bacterial interactions. The attachment of one bacterium to another (coaggregation) is likely to be crucial in the establishment of dental plaque (28, 38) and may be important in generating polymicrobial communities on the surface of and within epithelial cells (7) and in the invasion of dentinal tubules (33).

F. nucleatum is able to bind an extremely wide range of different bacteria as well as host cells and proteins. Remarkably, many of these interactions occur via one of two common mechanisms, L-arginine-sensitive and lactose-sensitive (13, 29, 32, 43–45, 48). In this report we have identified a novel L-arginine-sensitive interaction, the binding of S-IgA. Although adhesion of *F. nucleatum* to many diverse substrates is sensitive to L-arginine, subtle differences may exist. Attachment of fusobacteria to either *S. cristatus* or S-IgA did differ with respect to inhibition by EDTA. Coaggregation was insensitive but S-IgA-mediated agglutination was partially sensitive. Despite this, both interactions appear to be mediated by a single, high-molecular-weight protein. This protein did not appear to mediate lactose-sensitive interactions because coaggregation of *P. gingivalis* with isolate 21 was the same as with wild-type fusobacteria. In addition, we have previously shown that isolate 21 binds KB epithelial cells (a lactose-inhibitable interaction) at a similar level to wild-type (7). An arginine-binding protein of *F. nucleatum* of similar mass to arginine-binding protein has previously been implicated in coaggregation with oral streptococci. However, it was not characterized with respect to S-IgA binding and the protein was not identified (44). The recovery of arginine-binding protein from bacterial lysate by L-arginine beads provided a simple method of purification as well as demonstrating a strong affinity for this amino acid. Although we were able to demonstrate direct binding of *S. cristatus* and immunoglobulins to arginine-binding protein, the yield of purified arginine-binding protein was too low to examine whether this protein was capable of inhibiting coaggregation or S-IgA-mediated aggregation. We attempted to overcome this by making recombinant arginine-binding protein. Unfortunately, expression of arginine-binding protein in *Escherichia coli* proved to be toxic and we were unsuccessful.

The role of polar tufts of fimbriae on the surface of *S. cristatus* in mediating the coaggregation with *F. nucleatum* has been investigated in some detail (4, 16). Scanning electron microscopy confirmed the importance of these polar tufts of fimbriae in mediating coaggregation with *F. nucleatum*. Similar structures were not apparent on the fusobacteria and no morphological differences were seen between wild-type and isolate 21 (Data not shown). It is not clear whether arginine-binding protein binds these fibrils directly or indirectly.

The importance of genomics in the identification of a likely gene for arginine-binding protein cannot be understated. Researchers with an interest in *F. nucleatum* are fortunate that the genome sequences of all three sub-species are either complete or are in progress (6, 21, 22; sequencing of the genome of *F. nucleatum* ATCC 10953 is ongoing, see: http://www.hgsc.bcm.tmc.edu/projects/microbial/Fnucleatum/). Genome sequence analysis completed to date has identified several potential high-molecular-weight surface proteins (6, 21, 22). The SDS–PAGE analysis of *F. nucleatum* ATCC 10953 presented here revealed five proteins of mass >250 kDa. The reactivity of purified arginine-binding protein with immune serum, coupled with the loss of phenotype in isolate 21, provides good evidence that arginine-binding protein is both surface-exposed and immunogenic. Sequence analysis of arginine-binding protein is strongly indicative that this protein is a member of the autotransporter family of proteins, although we have no direct experimental evidence that this is the case. Autotransporter proteins are associated with a range of virulence functions, including adhesion, IgA protease, serum resistance and direct toxic effects. However, this is the first example of a role in coaggregation (arginine-binding protein exhibited no IgA protease activity – data not shown).

In this report we took a basic approach to genetic manipulation and selected for spontaneous mutants based on adhesive phenotype. Selection for an S-IgA non-binding phenotype yielded a number of isolates that were defective in this property. However, it is important to note that the selection of spontaneous mutants may result in the isolation of bacteria with more than one mutation. Although we have provided evidence that arginine-binding protein is central to coaggregation and immunoglobulin binding, specific genetic manipulations are required to confirm this. Fortunately, genetic techniques that have long been employed with other bacteria are beginning to become available for *F. nucleatum* (2, 12, 14, 26). Although the success of genetic manipulation varies between strains (12) these methods, coupled with the availability of complete genome sequences, will doubtless expand our understanding of *F. nucleatum* and, in particular, its surface proteins.

Acknowledgments

Ruoqiong Chen is acknowledged for her untiring technical assistance, Chris Frethem is acknowledged for his patient assistance with scanning electron microscopy and Kelly Johnston is acknowledged for assistance with development of coaggregation assays. The authors would like to take this opportunity to express their sadness at the sudden passing of Professor Stanley L. Erlandsen. This study was supported by USPHS grant DE 14214 from the National Institute of Dental and Craniofacial Research, Bethesda, MD 20892, USA. T.J.G. was supported by a summer research fellowship from Minn-CResT 5T32 DE 007288.

References

1. Altschul SF, Gish W, Miller W, Myers EW, Lipman DJ. Basic local alignment search tool. J Mol Biol 1990: **215**: 403–410.
2. Bachrach G, Haake SK, Glick A et al. Characterization of the novel *Fusobacterium nucleatum* plasmid pKH9 and evidence of an addiction system. Appl Environ Microbiol 2004: **70**: 6957–6962.
3. Bradshaw DJ, Marsh PD, Watson GK, Allison C. Role of *Fusobacterium nucleatum* and coaggregation in anaerobe survival in planktonic and biofilm oral microbial communities during aeration. Infect Immun 1998: **66**: 4729–4732.
4. Correia FF, DiRienzo JM, Lamont RJ, Anderman C, McKay TL, Rosan B. Insertional inactivation of binding determinants of *Streptococcus crista* CC5A using Tn916. Oral Microbiol Immunol 1995: **10**: 220–226
5. Dehazya P, Coles RS Jr. Agglutination of human erythrocytes by *Fusobacterium nucleatum*: factors influencing hemagglutination and some characteristics of the agglutinin. J Bacteriol 1980: **143**: 205–211.
6. Desvaux M, Khan A, Beatson SA, Scott-Tucker A, Henderson IR. Protein secretion systems in *Fusobacterium nucleatum*: genomic identification of Type 4 piliation and complete Type V pathways brings new insight into mechanisms of pathogenesis. Biochim Biophys Acta 2005: **1713**: 92–112.
7. Edwards AM, Grossman TJ, Rudney JD. *Fusobacterium nucleatum* transports noninvasive *Streptococcus cristatus* into human epithelial cells. Infect Immun 2006: **74**: 654–662.
8. Erlandsen SL, Kristich CJ, Dunny GM, Wells CL. High-resolution visualization of the microbial glycocalyx with low-voltage scanning electron microscopy: dependence on cationic dyes. J Histochem Cytochem 2004: **52**: 1427–1435.
9. Falkler WA Jr, Hawley CE. Hemagglutinating activity of *Fusobacterium nucleatum*. Infect Immun 1977: **15**: 230–238.
10. Grenier D, Michaud J. Demonstration of human immunoglobulin G Fc-binding activity in oral bacteria. Clin Diagn Lab Immunol 1994: **1**: 247–249.
11. Guo M, Han YW, Sharma A, De Nardin E. Identification and characterization of human immunoglobulin G Fc receptors of *Fusobacterium nucleatum*. Oral Microbiol Immunol 2000: **15**: 119–123.
12. Haake SK, Yoder SC, Attarian G, Podkaminer K. Native plasmids of *Fusobacterium nucleatum*: characterization and use in development of genetic systems. J Bacteriol 2000: **182**: 1176–1180.
13. Han YW, Shi W, Huang GT et al. Interactions between periodontal bacteria and human oral epithelial cells: *Fusobacterium nucleatum* adheres to and invades epithelial cells. Infect Immun 2000: **68**: 3140–3146.
14. Han YW, Ikegami A, Rajanna C et al. Identification and characterization of a novel adhesin unique to oral fusobacteria. J Bacteriol 2005: **187**: 5330–5340.
15. Handley P, Coykendall A, Beighton D, Hardie JM, Whiley RA. *Streptococcus crista* sp. nov., a viridans streptococcus with tufted fibrils, isolated from the human oral cavity and throat. Int J Syst Bacteriol 1991: **41**: 543–547.
16. Handley PS, Correia FF, Russell K, Rosan B, DiRienzo JM. Association of a novel high molecular weight, serine-rich protein (SrpA) with fibril-mediated adhesion of the oral biofilm bacterium *Streptococcus cristatus*. Oral Microbiol Immunol 2005: **20**: 131–140.
17. Henderson IR, Nataro JP. Virulence functions of autotransporter proteins. Infect Immun 2001: **69**: 1231–1243.
18. Henderson IR, Navarro-Garcia F, Nataro JP. The great escape: structure and function of the autotransporter proteins. Trends Microbiol 1998: **6**: 370–378.
19. Jakubovics NS, Kerrigan SW, Nobbs AH et al. Functions of cell surface-anchored antigen I/II family and Hsa polypeptides in interactions of *Streptococcus gordonii* with host receptors. Infect Immun 2005: **73**: 6629–6638.
20. Jensen HB, Skeidsvoll J, Fjellbirkeland A et al. Cloning of the fomA gene, encoding the major outer membrane porin of *Fusobacterium nucleatum* ATCC10953. Microb Pathog 1996: **21**: 331–342.
21. Kapatral V, Anderson I, Ivanova N et al. Genome sequence and analysis of the oral bacterium *Fusobacterium nucleatum* strain ATCC 25586. J Bacteriol 2002: **184**: 2005–2018.
22. Kapatral V, Ivanova N, Anderson I et al. Genome analysis of *F. nucleatum* sub spp *vincentii* and its comparison with the genome of *F. nucleatum* ATCC 25586. Genome Res 2003: **13**: 1180–1189.
23. Kaufman J, DiRienzo JM. Evidence for the existence of two classes of corncob (coaggregation) receptor in *Fusobacterium nucleatum*. Oral Microbiol Immunol 1988: **3**: 145–152.
24. Kaufman J, DiRienzo JM. Isolation of a corncob (coaggregation) receptor polypeptide from *Fusobacterium nucleatum*. Infect Immun 1989: **57**: 331–337.
25. Kinder SA, Holt SC. Localization of the *Fusobacterium nucleatum* T18 adhesin activity mediating coaggregation with *Porphyromonas gingivalis* T22. J Bacteriol 1993: **175**: 840–850.
26. Kinder Haake S, Yoder S, Gerardo SH. Efficient gene transfer and targeted mutagenesis in *Fusobacterium nucleatum*. Plasmid 2006: **55**: 27–38.
27. Kinder-Haake S, Lindemann, RA. *Fusobacterium nucleatum* T18 aggregates human mononuclear cells and inhibits their PHA-stimulated proliferation. J Periodontol 1997: **68**: 39–44.
28. Kolenbrander PE. Oral microbial communities: biofilms, interactions, and genetic systems. Annu Rev Microbiol 2000: **54**: 413–437.
29. Kolenbrander PE, Andersen RN. Inhibition of coaggregation between *Fusobacterium nucleatum* and *Porphyromonas* (*Bacteroides*) *gingivalis* by lactose and related sugars. Infect Immun 1989: **57**: 3204–3209.
30. Lafontaine ER, Wall D, Vanlerberg SL, Donabedian H, Sledjeski DD. *Moraxella catarrhalis* coaggregates with *Streptococcus pyogenes* and modulates interactions of *S. pyogenes* with human epithelial cells. Infect Immun 2004: **72**: 6689–6693.
31. Lancy P Jr, Dirienzo JM, Appelbaum B, Rosan B, Holt SC. Corncob formation between *Fusobacterium nucleatum* and *Streptococcus sanguis*. Infect Immun 1983: **40**: 303–309.
32. Levesque C, Lamothe J, Frenette M. Coaggregation of *Streptococcus salivarius* with periodontopathogens: evidence for involvement of fimbriae in the interaction with *Prevotella intermedia*. Oral Microbiol Immunol 2003: **18**: 333–337
33. Love RM, Malcolm D, McMillan D, Park Y, Jenkinson HF. Coinvasion of dentinal tubules by *Porphyromonas gingivalis* and *Streptococcus gordonii* depends upon binding specificity of streptococcal antigen I/II adhesin. Infect Immun 2000: **68**: 1359–1365.
34. Mager DL, Ximenez-Fyvie LA, Haffajee AD, Socransky SS. Distribution of selected bacterial species on intraoral surfaces. J Clin Periodontol 2003: **30**: 644–654.

35. Mangan DF, Novak MJ, Vora SA, Mourad J, Kriger PS. Lectinlike interactions of *Fusobacterium nucleatum* with human neutrophils. Infect Immun 1989: **57**: 3601–3611.
36. Marchler-Bauer A, Anderson JB, Cherukuri PF et al. CDD: a Conserved Domain Database for protein classification. Nucleic Acids Res 2005: **33** Database Issue: D192–D196.
37. Ozaki M, Miyake Y, Shirakawa M, Takemoto T, Okamoto H, Suginaka H. Binding specificity of *Fusobacterium nucleatum* to human erythrocytes, polymorphonuclear leukocytes, fibroblasts, and HeLa cells. J Periodontal Res 1990: **25**: 129–134.
38. Rickard AH, Gilbert P, High NJ, Kolenbrander PE, Handley PS. Bacterial coaggregation: an integral process in the development of multi-species biofilms. Trends Microbiol 2003: **11**: 94–100.
39. Rudney JD, Strait CA. Effects of *Streptococcus crista* and human saliva on the viability of *Fusobacterium nucleatum* ATCC 10953. Arch Oral Biol 2000: **45**: 667–674.
40. Rudney JD, Chen R, Sedgewick GJ. Intracellular *Actinobacillus actinomycetemcomitans* and *Porphyromonas gingivalis* in buccal epithelial cells collected from human subjects. Infect Immun 2001: **69**: 2700–2707.
41. Rudney JD, Chen R, Zhang G. Streptococci dominate the diverse flora within buccal cells. J Dent Res 2005: **84**: 1165–1171.
42. Rudney JD, Chen R, Sedgewick GJ. *Actinobacillus actinomycetemcomitans*, *Porphyromonas gingivalis*, and *Tannerella forsythensis* are components of a polymicrobial intracellular flora within human buccal cells. J Dent Res 2005: **84**: 59–63.
43. Shaniztki B, Hurwitz D, Smorodinsky N, Ganeshkumar N, Weiss EI. Identification of a *Fusobacterium nucleatum* PK1594 galactose-binding adhesin which mediates coaggregation with periopathogenic bacteria and hemagglutination. Infect Immun 1997: **65**: 5231–5237.
44. Takemoto T, Ozaki M, Shirakawa M, Hino T, Okamoto H. Purification of arginine-sensitive hemagglutinin from *Fusobacterium nucleatum* and its role in coaggregation. J Periodontal Res 1993: **28**: 21–26.
45. Takemoto T, Hino T, Yoshida M, Nakanishi K, Shirakawa M, Okamoto H. Characteristics of multimodal co-aggregation between *Fusobacterium nucleatum* and streptococci. J Periodontal Res 1995: **30**: 252–257.
46. Trüper HG, Clari D'C. Taxonomic note: necessary correction of specific epithets formed as substantives (nouns) "in apposition". Int J Syst Bacteriol 1997: **47**: 908–909.
47. Tuttle RS, Mangan DF. Interaction of *Fusobacterium nucleatum* 191 with human peripheral blood lymphocytes. J Periodontal Res 1990: **25**: 364–371.
48. Tuttle RS, Strubel NA, Mourad J, Mangan DF. A non-lectin-like mechanism by which *Fusobacterium nucleatum* 10953 adheres to and activates human lymphocytes. Oral Microbiol Immunol 1992: **7**: 78–83.
49. Weiss EI, Shaniztki B, Dotan M, Ganeshkumar N, Kolenbrander PE, Metzger Z. Attachment of *Fusobacterium nucleatum* PK1594 to mammalian cells and its coaggregation with periodontopathogenic bacteria are mediated by the same galactose-binding adhesin. Oral Microbiol Immunol 2000: **15**: 371–377.
50. Xie H, Gibbons RJ, Hay DI. Adhesive properties of strains of *Fusobacterium nucleatum* of the subspecies *nucleatum*, *vincentii* and *polymorphum*. Oral Microbiol Immunol 1991: **6**: 257–263.